Diffraction of Gaussian and Laguerre–Gauss beams from a circular aperture using the moment expansion method

K. Dupraz, A. Martens, J.M. Rax, F. Zomer

Diffraction of Gaussian and Laguerre-Gauss beams from a circular aperture using the moment expansion method

K. DUPRAZ[1], A. MARTENS[1,*], J.M. RAX[1], AND F. ZOMER[1]

[1] Université Paris-Saclay, CNRS/IN2P3, IJCLab, 91405 Orsay, France
[*] Corresponding author: aurelien.martens@ijclab.in2p3.fr

Compiled October 10, 2023

A method based on the distribution theory is introduced to compute the Fresnel diffraction integral. It is applied to the diffraction of Gaussian and Laguerre-Gauss beams by a circular aperture. Expressions of the diffracting field are recast into perturbation series describing the near and far field regions.

http://dx.doi.org/10.1364/ao.XX.XXXXXX

1. INTRODUCTION

Laguerre-Gauss Beams (LGB) carry angular momentum and are used in a wide field of research [1]. Recently, it has been used in research topics as different as generation of elegant elliptical vortex Hermite–Gaussian beams [2], non-linear optics [3], underwater optical communications and [4] plasma physics [5].

Explicit formula, easy to handle and fast to compute, describing the propagation and diffraction of LGB are needed to model their interactions with various media. However, whereas diffraction of Gaussian Beams (GB) or plane waves has extensively been studied in the past, LGB have received less attention. See, for instance, [6–8] and references therein.

Unlike previous methods [7] used to compute Fresnel diffraction integrals, here we use the theory of distributions. Since these integrals can be written as Fourier and Hankel transforms [9], we show that the moment expansion method [10] permits the accurate derivation of near and far field diffraction. This method has been used in statistical physics and quantum optics [10] but never, to the best of our knowledge, in diffracting optics. As we show, it leads to easy calculations of diffraction integrals and could also be useful to solve similar problems. Our result for LGB diffraction in the far-field region, while supported by the numerical calculations of Fresnel integrals, is found to be in disagreement with the published result of [6].

This article is organized as follows. The Fresnel integral and a derivation of an expression for the n^{th} order derivative of the Dirac distribution in polar coordinates are presented in section 2. This latter mathematical tool is a key element of moment expansions. To the best of our knowledge, its use in this context has not yet been published. In section 3 we show how the moment expansion method applied to diffraction integrals of GB by a circular aperture can be recast into perturbation expansions describing near and far fields of the diffracted beam. Section 4 is eventually devoted to LGB.

2. FORMALISM

Diffraction of an electromagnetic field by a circular aperture of radius a is addressed in this article. We restrict ourselves to the large aperture limit $a \gg \lambda$, where λ is the wavelength, so that scalar field theory can be used [11]. Paraxial approximation is further assumed to describe the scalar field propagation along an axis labeled z. This axis is normal to the aperture plane and intersects this plane at the center of the circular aperture. The transverse coordinates in the aperture plane, located at $z = 0$ and in the observation plane located at $z > 0$ are written x', y' and x, y respectively.

For a paraxial scalar monochromatic field $\mathcal{E}(\mathbf{r}, t) = E(\mathbf{r}) \exp(-i\omega_0 t)$, with ω_0 the angular frequency and $\mathbf{r}^t = (x, y, z)$, the Fresnel diffraction integral for $E(\mathbf{r})$ is given by [9]:

$$\begin{aligned} E(\mathbf{r}) &= \frac{\exp(ikz)}{i\lambda z} \exp\left[i\frac{k}{2z}(x^2+y^2)\right] \\ &\quad \int\int_{-\infty}^{+\infty} E(x',y',0) \exp\left[i\frac{k}{2z}(x'^2+y'^2)\right] \\ &\quad \exp\left[-i(x'\omega_x + y'\omega_y)\right] \mathrm{d}x'\mathrm{d}y' \end{aligned} \quad (1)$$

where $k = 2\pi/\lambda$, $\omega_x = kx/z$ and $\omega_y = ky/z$. Mathematical properties of the Fresnel integral are well known (e.g. see [12]) as well as its range of applicability (e.g. see [13]).

For a circular aperture, one uses polar coordinates so that, assuming a circular symmetry of the wave-front of the incident field, Eq. 1 can be written as a Hankel transform [9, 14]

$$E(\rho, z) = \frac{\exp(ikz)}{i\lambda z} \exp\left[i\frac{k}{2z}\rho^2\right] 2\pi\mathcal{I}(\rho) \quad (2)$$

with

$$\mathcal{I}(\rho) = \int_0^{+\infty} \mathrm{circ}(\rho'/a) E(\rho', 0) \exp\left[i\frac{k}{2z}\rho'^2\right] J_0(\tilde{\rho}\rho')\rho' \mathrm{d}\rho' \quad (3)$$

where J_0 is the zeroth order Bessel function of the first kind, $\rho' = \sqrt{x'^2+y'^2}$, $\rho = \sqrt{x^2+y^2}$, $\tilde{\rho} = \sqrt{\omega_x^2+\omega_y^2} = k\rho/z$ and

$\mathrm{circ}(\rho'/a) = 1$ if $\rho' \leq a$ and 0 if $\rho' > a$. Modifications of Eq. 3 for a non-circular symmetric incident field are given in section 4.

Eq. 3 thus reads [15]

$$\mathcal{I}(\rho) = \mathcal{H}_0\Big[f(\rho')g(\rho')\Big] \tag{4}$$

where $f(\rho') = \mathrm{circ}(\rho'/a)$, $g(\rho') = E(\rho',0)\exp\Big[ik\rho'^2/(2z)\Big]$ and where $\mathcal{H}_0$ stands for the zeroth order Hankel transform. That is

$$\tilde{f}(\tilde{r}) = \mathcal{H}_n[f(r)] = \int_0^\infty f(r)J_n(\tilde{r}r)r\mathrm{d}r \tag{5}$$

with $n = 0$.

Using $\mathcal{H}_n[\mathcal{H}_n[f(r)]] = f(r)\ \forall n$ one can write Eq. 4 in two equivalent ways:

$$\mathcal{I}(\rho) = \begin{cases} \mathcal{H}_0[\mathcal{H}_0[\tilde{g}(\tilde{u})]f(\rho')] \\ \text{or} \\ \mathcal{H}_0[\mathcal{H}_0[\tilde{f}(\tilde{u})]g(\rho')] \end{cases} \tag{6}$$

In order to compute the integral of Eq. 4, we choose to perform a moment expansion of either $\tilde{g}(\tilde{u})$ or $\tilde{f}(\tilde{u})$ in the first or second expression of Eq. 6, respectively. Though they should lead to the same results, it comes out that it either corresponds to the near or far field approximations when truncating the moment expansion.

Making a moment expansion of function $\tilde{g}(\tilde{u})$, that is the Hankel transform of the incident field $E(\rho',0)$ times the Fresnel propagator term $\exp[ik\rho'^2/(2z)]$, therefore leads to the diffracted far field. Whereas expanding the smooth function $\tilde{f}(\tilde{u})$, *i.e.* the Hankel transform of the screen aperture function, multiplied by a Gaussian regulation function leads to the diffracted near field. These two calculations will therefore be addressed separately in the following sections 3 and 4. Eventually, it is worth mentioning that one cannot compute directly the moment expansion of $f(\rho')g(\rho')$ in Eq. 4 since no formal expression exists for it and that we are only expanding smooth functions in moments.

A. Moment expansion in polar coordinates

We define the moments of a function $h(r,\theta)$ in polar coordinates (r,θ) by

$$\mu_{mn} = \int_0^{2\pi}\int_0^{+\infty} h(r,\theta)r^m\exp(in\theta)r\mathrm{d}r\mathrm{d}\theta \tag{7}$$

with $x = r\cos\theta$ and $y = r\sin\theta$ and $m \in \mathbb{N}$, $n \in \mathbb{Z}$. Following [10], we then seek for a moment expansion of $h(r,\theta)$ as a function of the n-order derivatives of the Dirac distribution $\delta^{[n]}(r)$. A derivation of the first-order derivative can be found in [16]. Defining $\int_0^{+\infty}\delta(r)\mathrm{d}r = 1$ one has $\int_0^{+\infty}\delta^{[1]}(r)f(r)r\mathrm{d}r = -f(0)$. However, to the best of our knowledge, the n^{th}-order derivatives are not available in the existing literature. Thus, we need to determine for any $r_0 \geq 0$

$$F_n(r_0) = \int_0^{+\infty}\delta^{[n]}(r-r_0)f(r)r\mathrm{d}r. \tag{8}$$

To do so, we extend a method used in [16]. Let $g(r)$ be a function having a definite n^{th}-order derivative. It is defined by the following limit

$$g^{[n]}(r) = \lim_{\epsilon\to 0}\frac{1}{\epsilon^n}D_c^{[n]}\{g\}(r,\epsilon) \tag{9}$$

where $D_c^{[n]}\{g\}(r,\epsilon)$ is the n^{th} order centered finite difference [17]

$$D_c^{[n]}\{g\}(r,\epsilon) = \sum_{k=0}^{n}(-1)^k\frac{n!}{k!(n-k)!}g\left(r+\left[\frac{n}{2}-k\right]\epsilon\right). \tag{10}$$

Replacing $g(r)$ by $\delta(r-r_0)$ and injecting it in Eq. 8, one obtains

$$\begin{aligned} F_n(r_0) &= \lim_{\epsilon\to 0}\frac{1}{\epsilon^n}\sum_{k=0}^{n}(-1)^k\frac{n!}{k!(n-k)!} \\ &\quad \left(r_0-\left[\frac{n}{2}-k\right]\epsilon\right)f(r_0-\left[\frac{n}{2}-k\right]\epsilon) \\ &= r_0(-1)^n f^{[n]}(r_0) + \\ &\quad \lim_{\epsilon\to 0}\frac{n(-1)^n}{\epsilon^{n-1}}D_c^{[n-1]}\{f\}\left(r_0+\frac{\epsilon}{2},\epsilon\right) \\ &= r_0(-1)^n f^{[n]}(r_0) + n(-1)^n f^{[n-1]}(r_0). \end{aligned} \tag{11}$$

It should be noted that this expression differs significantly from that in Cartesian coordinates [10]. The moment expansion of $h(r,\theta)$ is defined by

$$h(r,\theta) = \frac{1}{2\pi}\sum_{n=-\infty}^{+\infty}\sum_{m=0}^{+\infty}\frac{(-1)^{m+1}}{(m+1)!}\mu_{mn}\exp(-in\theta)\delta^{[m+1]}(r). \tag{12}$$

For a radially symmetric function, only the term $n = 0$ in the above sum remains. Therefore, $h(r,\theta) \equiv h(r)$ and the previous equation simplifies to

$$h(r) = \frac{1}{2\pi}\sum_{m=0}^{+\infty}\frac{(-1)^{m+1}}{(m+1)!}\mu_m\delta^{[m+1]}(r) \tag{13}$$

with $\mu_m = 2\pi\int_0^{+\infty}h(r)r^m r\mathrm{d}r$. Such a series expansion for the function $h(r)$ is suitable because it is going to be inserted inside an integral over r.

3. GAUSSIAN BEAM

Here, the incident field of Eq. 3 reads $E(\rho',0) = E_0\exp(-\rho'^2/w_0^2)$ where w_0 is the beam waist. Following [6], we thus fix the waist position in the aperture plane $z = 0$. One therefore gets $g(\rho') = E_0\exp\Big[-\alpha\rho'^2\Big]$ with

$$\alpha = \frac{1}{w_0^2}\left(1-i\frac{z_R}{z}\right) = \frac{1}{w_0^2}-i\frac{\pi N_F}{a^2} \tag{14}$$

where we have introduced two important parameters, the Rayleigh range $z_R = \pi w_0^2/\lambda$ and the Fresnel number $N_F = a^2/(\lambda z)$.

A. Far field and collimated beam region

We start with the first expression of Eq. 6:

$$\begin{aligned} \mathcal{I}(\rho,z) &= \mathcal{H}_0\Big[\mathcal{H}_0[\tilde{g}(\tilde{\rho}_0)]f(r)\Big] \\ &= \int_0^\infty\tilde{g}(\tilde{\rho_0})\int_0^a J_0(r\tilde{\rho_0})J_0(r\tilde{\rho})r\mathrm{d}r\tilde{\rho_0}\mathrm{d}\tilde{\rho_0} \end{aligned} \tag{15}$$

For $\tilde{\rho} \neq \tilde{\rho_0}$, the integral over r is known, see p. 664 of [18], we then get

$$\begin{aligned} \mathcal{I}(\rho,z) &= a^2\int_0^\infty\tilde{\rho_0}\tilde{g}(\tilde{\rho_0}) \\ &\quad \frac{\Big(\tilde{\rho}_{0r}J_1(\tilde{\rho_0}_r)J_0(\tilde{\rho}_r)-\tilde{\rho}_r J_1(\tilde{\rho}_r)J_0(\tilde{\rho_0}_r)\Big)}{\tilde{\rho}_{0r}^2-\tilde{\rho}_r^2}\mathrm{d}\tilde{\rho_0} \end{aligned} \tag{16}$$

with $\tilde{\rho}_{0r} = a\tilde{\rho}_0$ and $\tilde{\rho}_r = a\tilde{\rho}$. A formal expression also exits for $\tilde{\rho} = \tilde{\rho}_0$ but it turns out that our final result will be finite in the limit $\tilde{\rho} \to \tilde{\rho}_0 = 0$ using Eq. 16. We will therefore extend the use of Eq. 16 to this limit.

Using the results of section 2.A for $\tilde{g}(\tilde{\rho}_0) = E_0 \exp[-\tilde{\rho_0}^2/(4\alpha)]/(2\alpha)$, we get

$$\tilde{g}(\tilde{\rho}_0) = E_0 \sum_{n=0}^{\infty} \frac{(-1)^{n+1}}{(n+1)!} 2^n \alpha^{n/2} \Gamma\left(\frac{n}{2}+1\right) \delta^{[n+1]}(\tilde{\rho}_0) \qquad (17)$$

Inserting this expression into Eq. 16 and performing the integration over $\tilde{\rho}_0$, one obtains

$$\begin{aligned} \mathcal{I}(\rho) \quad = \quad & a^2 E_0 \frac{J_1(\tilde{\rho}_r)}{\tilde{\rho}_r} + a^2 E_0 \sum_{n=1}^{\infty} \frac{2^n}{n!} \Gamma\left(\frac{n}{2}+1\right) (a^2\alpha)^{n/2} \\ & \left[\frac{\partial^n}{\partial \tilde{\rho}_{0r}^n} \left(\frac{\tilde{\rho}_{0r} J_1(\tilde{\rho}_{0r})}{\tilde{\rho}_{0r}^2 - \tilde{\rho}_r^2} \right) \Big|_{\tilde{\rho}_{0r}=0} J_0(\tilde{\rho}_r) \right. \\ & \left. - \frac{\partial^n}{\partial \tilde{\rho}_{0r}^n} \left(\frac{J_0(\tilde{\rho}_{0r})}{\tilde{\rho}_{0r}^2 - \tilde{\rho}_r^2} \right) \Big|_{\tilde{\rho}_{0r}=0} \tilde{\rho}_r J_1(\tilde{\rho}_r) \right]. \end{aligned} \qquad (18)$$

The first term of the r.h.s. of this equation is the solution of the Fraunhofer diffraction integral [9] which corresponds to the limits $a/w_0 \to 0$ and $N_F \to 0$. Eq. 18 is an expansion in powers of $(a^2\alpha)$ and can then be viewed as a perturbation expansion for $a^2|\alpha| \lesssim 1$. Therefore, Eq. 18 can be used either if $a/w_0 \ll 1$ and $N_F \lesssim 1/\pi$ or $N_F \ll 1/\pi$ and $a/w_0 \lesssim 1$.

Expanding the n^{th}-order partial derivatives terms of Eq. 18 one sees that the sum vanishes for odd values n. Eq. 18 can thus be written

$$\mathcal{I}(\rho, z) = \mathcal{I}^{[0]}(\rho, z) + \sum_{p=1}^{\infty} \mathcal{I}^{[p]}(\rho, z) \qquad (19)$$

with $\mathcal{I}^{[0]} = a^2 E_0 J_1(\tilde{\rho}_r)/\tilde{\rho}_r$ and

$$\begin{aligned} \mathcal{I}^{[p]}(\rho, z) \quad = \quad & a^2 E_0 2^{2p} p! (a^2\alpha)^p \\ & \left[J_1(\tilde{\rho}_r) \sum_{k=0}^{p} \frac{(-1)^k \tilde{\rho}_r^{2k-2p-1}}{(k)!^2 2^{2k}} \right. \\ & \left. - J_0(\tilde{\rho}_r) \sum_{k=0}^{p-1} \frac{(-1)^k \tilde{\rho}_r^{2k-2p}}{(k)!(k+1)! 2^{2k+1}} \right]. \end{aligned} \qquad (20)$$

This expression shows that the limit

$$\lim_{\tilde{\rho}_r \to 0} \mathcal{I}^{[p]}(\rho) = E_0 \frac{a^2 (-1)^p (a^2\alpha)^p}{2(p+1)!}, \qquad (21)$$

which corresponds to the case $\tilde{\rho}_r = \tilde{\rho}_{0r} = 0$ in Eq. 16, is in fact finite for all p.

By numerically evaluating Eq. 19 one has to truncate the series over p. Accordingly, a cutoff parameter $p_{max} = \text{Max}(p)$ must then be introduced and the numerical accuracy can be estimated simply by computing $\mathcal{I}^{[p_{max}+1]}(\rho)$. As for the speed convergence of Eq. 19, it depends on a/w_0, N_F and on the range of $\tilde{\rho}_r$. This must be addressed numerically on a case by case basis (as for the other results of this article). To illustrate that, numerical calculations were performed taking $a = 1$, $N_F = 0.1$ and $a/w_0 = 1$. Fig. 1 shows a comparison between the numerical integration of Eq. 4 done using the rectangle method, the zeroth order ($p_{max} = 0$) and the sixth order ($p_{max} = 6$) approximations of Eq. 19. Whereas the zeroth order approximation is not precise enough, taking only six terms in the series of Eq. 19 leads to a good agreement. To quantify the numerical precision one defines

$$\mathcal{R}_{p_{max}}(\rho, z) = \frac{\mathcal{I}^{[p_{max}+1]}(\rho, z)}{\mathcal{I}^{[0]}(\rho, z) + \sum_{p=1}^{p_{max}} \mathcal{I}^{[p]}(\rho, z)} \qquad (22)$$

that is the relative next order contribution for a given p_{max} value. Fig. 2 shows the values of $\mathcal{R}$ as a function of $a\tilde{\rho}$ for various values of p_{max} and for the same parameters as in Fig. 1. The curve for $p_{max} = 0$ corresponds to the correction to the Fraunhofer approximation. Since here $N_F = 0.1$ is sizable, such a large correction is expected. As p_{max} increases one sees that the precision also increases. It is however dependent on the value of $a\tilde{\rho}$.

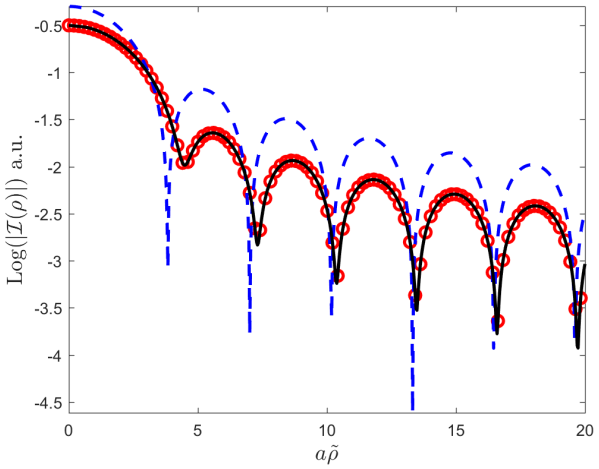

Fig. 1. $\mathcal{I}(\rho)$ as a function of the dimensionless variable $a\tilde{\rho}$ for $a = 1$, $N_F = 0.1$ and $a/w_0 = 1$. Dashed line: zeroth order ($p_{max} = 0$ in Eq. 19); full line : 6^{th} order ($p_{max} = 6$ in Eq. 19) ; circles: numerical integration (Eq. 4).

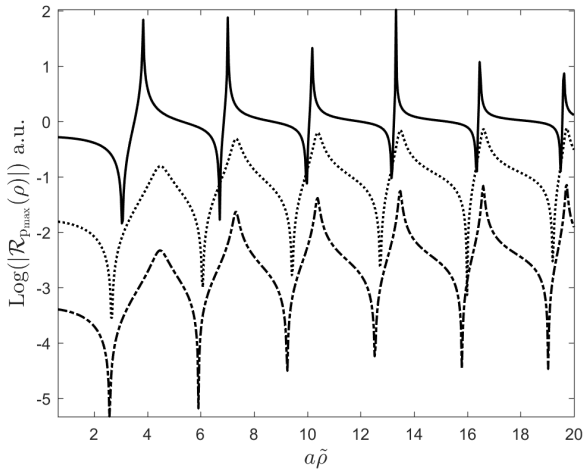

Fig. 2. $\mathcal{R}_{p_{max}}(\rho)$ as a function of the dimensionless variable $a\tilde{\rho}$ for $a = 1$, $N_F = 0.1$ and $a/w_0 = 1$. Full line: zeroth order $p_{max} = 0$; dotted line: $p_{max} = 3$; dashed-dotted: $p_{max} = 5$.

B. Near field and focused beam region

We start start with the second expression of Eq. 6:

$$\begin{aligned}\mathcal{I}(\rho) &= \mathcal{H}_0\Big[\mathcal{H}_0[\tilde{f}(\tilde{\rho}_0)]g(r)\Big] \\ &= E_0\int_0^\infty \tilde{f}(\tilde{\rho_0})\int_0^\infty \exp(-\alpha r^2)J_0(r\tilde{\rho_0})J_0(r\tilde{\rho})r\mathrm{d}r\tilde{\rho_0}\mathrm{d}\tilde{\rho_0}\end{aligned}$$

Performing the integral over r, see p. 707 of [18], we obtain

$$\begin{aligned}\mathcal{I}(\rho) &= \frac{E_0}{2\alpha}\exp\left(-\frac{\tilde{\rho}^2}{4\alpha}\right)\int_0^\infty \tilde{f}(\tilde{\rho_0}) \\ &\quad \exp\left(-\frac{\tilde{\rho}_0^2}{4\alpha}\right)I_0\left(\frac{\tilde{\rho_0}\tilde{\rho}}{2\alpha}\right)\tilde{\rho_0}\mathrm{d}\tilde{\rho_0} \qquad (23)\end{aligned}$$

where I_0 is the zeroth order modified Bessel function of the first kind. However, it turns out that the moments of $\tilde{f}(\tilde{\rho_0}) = aJ_1(a\tilde{\rho_0})/\tilde{\rho_0}$ are not defined. Since the moments of

$$\tilde{f}_q(\tilde{\rho_0}) = aJ_1(a\tilde{\rho_0})/\tilde{\rho_0}\exp(-q\tilde{\rho}_0^2/(4\alpha))$$

are well defined for $0 < q \leq 1$ and $\Re(\alpha) > 0$, we can rewrite Eq. 23

$$\begin{aligned}\mathcal{I}(\rho) &= \frac{E_0}{2\alpha}\exp\left(-\frac{\tilde{\rho}^2}{4\alpha}\right)\int_0^\infty \tilde{f}_q(\tilde{\rho_0}) \\ &\quad \exp\left(-(1-q)\frac{\tilde{\rho}_0^2}{4\alpha}\right)I_0\left(\frac{\tilde{\rho_0}\tilde{\rho}}{2\alpha}\right)\tilde{\rho_0}\mathrm{d}\tilde{\rho_0} \qquad (24)\end{aligned}$$

and perform a moment expansion of $\tilde{f}_q(\tilde{\rho_0})$.

Taking $q = 1$ we indeed obtain a very compact solution. Using the results of section 2.A, we get, see p. 706 of [18]

$$\begin{aligned}\tilde{f}_1(\tilde{\rho_0}) &= \frac{1}{a}\exp\left(-\frac{a^2\alpha}{2}\right)\sum_{n=0}^\infty M_{n/2,1/2}(a^2\alpha) \\ &\quad \frac{(-1)^{n+1}2^n\alpha^{n/2}\Gamma(1+n/2)}{(n+1)!}\delta^{[n+1]}(\tilde{\rho_0}) \qquad (25)\end{aligned}$$

where $M_{n/2,1/2}(X)$ is the Whittaker M function, see p. 1024 of [18]. Inserting this expression into Eq. 24 and performing the integration over $\tilde{\rho_0}$, we obtain

$$\begin{aligned}\mathcal{I}(\rho) &= \frac{E_0}{2\alpha}\exp\left(-\frac{\tilde{\rho}^2}{4\alpha}\right)\exp\left(-\frac{a^2\alpha}{2}\right) \\ &\quad \sum_{n=0}^\infty \frac{M_{n,1/2}(a^2\alpha)}{2^{2n}n!}\left(\frac{1}{a^2\alpha}\right)^n\tilde{\rho}_r^{2n} \qquad (26)\end{aligned}$$

here we used $\partial^n/\partial X^n[I_0(YX)] = (2n)!/(2^{2n}n!^2)Y^{2n}$ for $X = 0$. Eq. 26 is an expansion in power of $1/(a\alpha)$. If $a/w_0 \gg 1$ ($N_F \gg 1/\pi$), Eq. 26 will thus be useful for $N_F \gtrsim 1/\pi$ ($a/w_0 \gtrsim 1$). As in the previous section, we can write Eq. 26 in the form of Eq. 19 with

$$\mathcal{I}^{[p]}(\rho,z) = \frac{E_0}{2\alpha}\exp\left(-\frac{\tilde{\rho}^2}{4\alpha}\right)\exp\left(-\frac{a^2\alpha}{2}\right)\frac{M_{p,1/2}(a^2\alpha)\tilde{\rho}_r^{2p}}{2^{2p}p!(a^2\alpha)^p}. \qquad (27)$$

From these two expressions one can further use Eq. 22 to define $\mathcal{R}_{p_{max}}(\rho,z)$ for the far-field region, where $p_{max} = \mathrm{Max}(p)$.

Figure 3 shows $\mathcal{I}(\rho)$ as a function of the dimensionless variable $a\tilde{\rho}$ for $a = 1$, $N_F = 10$ and $a/w_0 = 5/4$. For this set of parameters and the range $a\tilde{\rho} \leq 30$, it was necessary to take $p_{max} = 60$ to match the numerical integration of Eq. 4. $\mathcal{R}_{p_{max}}$ is shown in Fig. 4 as a function of $a\tilde{\rho}$ for various values of p_{max} and

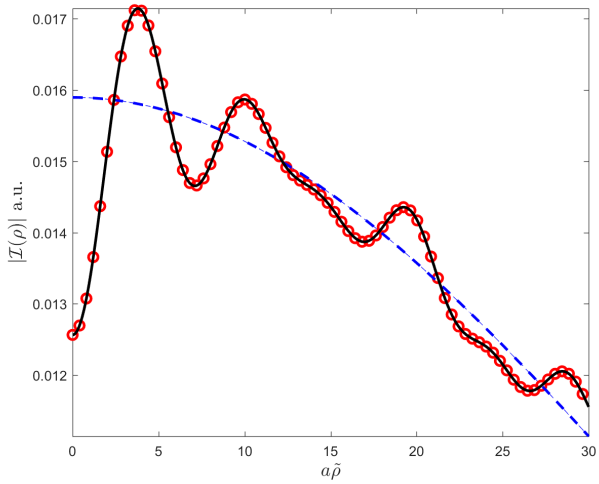

Fig. 3. $\mathcal{I}(\rho)$ as a function of the dimensionless variable $a\tilde{\rho}$ for $a = 1$, $N_F = 10$ and $a/w_0 = 5/4$. Dashed line: zeroth order ($n = 0$ contribution in Eq. 26); full line: 60^{th} order ($p_{max} = 60$ in Eq. 26); circles: numerical integration (Eq. 4).

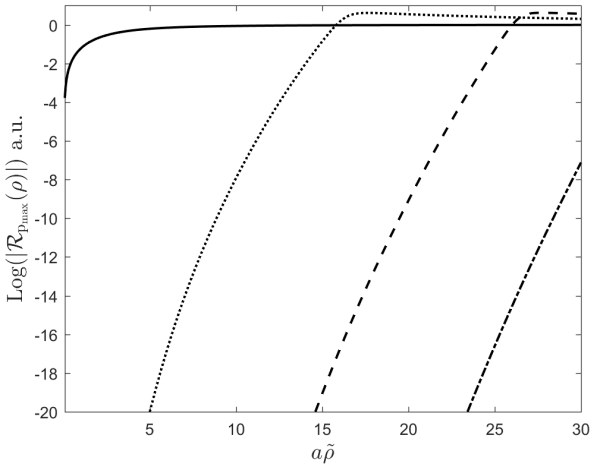

Fig. 4. $\mathcal{R}_{p_{max}}(\rho)$ as a function of the dimensionless variable $a\tilde{\rho}$ for the same parameter as in Fig. 3. Full line: $p_{max} = 0$; Dotted line: $p_{max} = 19$; Dashed line: $p_{max} = 39$; Dashed-dotted: $p_{max} = 59$.

for the same parameters as in Fig. 3. As for the far field case of the previous section, the precision strongly depends on p_{max} and decreases as $a\tilde{\rho}$ increases. Here much more terms are needed to reach accurate calculations and one even gets $\mathcal{R}_{p_{max}} > 1$ for some $a\tilde{\rho}$ intervals, e.g. for $p_{max} = 19$ if $a\tilde{\rho} > 15$ in Fig. 4.

We checked numerically that the range of validity of Eq. 26 with respect to the parameters a/w_0 and N_F was indeed sizable provided that the tuning of p_{max} can be flexible enough. For $a/w_0 \gtrapprox 1$ we could vary N_F over a large range $10^{-2} \lessapprox N_F \lessapprox 10^4$. The limits for larger values of N_F and smaller values of a/w_0 comes from the numerical evaluation of the special function $M_{n,1/2}(X)$ and from the factorial term for large p_{max} values. These can be evaluated to arbitrary precision at the price of increasing computing time to prohibitive values.

Eventually, it is instructive here to write the expression of the corresponding electric field of Eq. 2:

$$E(\rho) = \sqrt{\frac{2}{\pi}}\frac{q(0)}{w_0 q(z)}\exp\left(-\frac{ik\rho^2}{2q(z)}\right)\exp(ikz) \exp\left(-\frac{a^2\alpha}{2}\right)\sum_{n=0}^{\infty}\frac{(\pi N_F)^{2n}M_{n,1/2}(a^2\alpha)}{(a^2\alpha)^n n!}\rho_r^{2n} \quad (28)$$

with $E_0 = \sqrt{2/\pi}/w_0$, $q(z) = z - iz_R$ and $z_R = \pi w_0^2/\lambda$. Using $\lim_{\Re(X)\to\infty}\exp(-X/2)M_{0,1/2}(X) = 1$, one sees that for $n = 0$ and $a/w_0 \gg 1\,\forall z$, Eq. 28 gives the expression of the paraxial Gaussian beam [19]. Beside, for $a/w_0 \lessapprox 1$ and in the near field limit $N_F \gg 1$, one can use the asymptotic expansion of $M_{0,1/2}(X)$ for $|X| \gg 1$ [20] to get a very compact expression

$$E(\rho) \approx \sqrt{\frac{2}{\pi}}\frac{q(0)}{w_0 q(z)}\exp\left(-\frac{ik\rho^2}{2q(z)}\right)\exp(ikz) \left[1 - \exp(-a^2\alpha)J_0(a\rho)\right]. \quad (29)$$

This expression is valid in the very near field region where the Fresnel approximation holds [21] but not in the shadow region. It is also complementary to other results obtained with plane waves [22].

4. LAGUERRE-GAUSS BEAM

For an incident Laguerre-Gauss beam [19] one has $E_{p,\ell}(\rho',\theta',0) = \mathcal{F}_{p,\ell}(\rho')\exp(-i\ell\theta')$, with

$$\mathcal{F}_{p,\ell}(\rho') = E_0\left(\frac{\rho'\sqrt{2}}{w_0}\right)^{|\ell|}\mathrm{L}_p^{|\ell|}\left(\frac{2\rho'^2}{w_0^2}\right)\exp\left(-\frac{\rho'^2}{w_0^2}\right) \quad (30)$$

where $\mathrm{L}_n^{|\ell|}(X)$ is the generalized Laguerre polynomial, see p. 1000 of [18], with $\ell \in \mathbb{Z}$, $p \in \mathbb{N}$ and $x' = \rho'\cos\theta'$, $y' = \rho'\sin\theta'$. Eq. 3 now reads

$$E_{p,\ell}(\rho,\theta,z) = \frac{\exp(ikz)}{i\lambda z}\exp\left[i\frac{k}{2z}\rho^2\right] 2\pi i^{-\ell}\exp(i\ell\theta)\mathcal{I}_{p,\ell}(\rho,z) \quad (31)$$

with $x = \rho\cos\theta$, $y = \rho\sin\theta$ and

$$\mathcal{I}_{p,\ell}(\rho,z) = \int_0^{\infty}\mathrm{circ}\left(\frac{\rho'}{a}\right)\mathcal{F}_{p,\ell}(\rho')\exp\left(i\pi N_F\frac{\rho'^2}{a^2}\right)J_\ell(\tilde{\rho}\rho')\rho'\mathrm{d}\rho' \quad (32)$$

Eq. 32 can be further written in the form

$$\mathcal{I}_{p,\ell}(\rho,z) = \mathcal{H}_\ell\left\{\mathcal{H}_0\mathcal{H}_0\left[f(\rho')\right]\mathcal{H}_\ell\mathcal{H}_\ell\left[G(\rho')\right]\right\} \quad (33)$$

with $f(\rho') = \mathrm{circ}(\rho'/a)$, $G(\rho') = \mathcal{F}_{p,\ell}(\rho')\exp(iN_F\rho'^2/a^2)$ and where $\mathcal{H}_\ell[X]$ is the ℓth-order Hankel transform with $\mathcal{H}_\ell[X] = \mathcal{H}_\ell^{-1}[X]$. This expression, together with the phase factor $\exp(i\ell\theta)$ of Eq. 31, corresponds to the convolution product of non circularly symmetric functions in polar coordinates [23].

A. Far field and collimated beam region

As in section 3.A, we first evaluate the following integral

$$\mathcal{I}_{p,\ell}(\rho,z) = \mathcal{H}_\ell\left\{f(\rho')\mathcal{H}_\ell\left[\tilde{G}(\tilde{\rho}_0)\right]\right\} = \int_0^{\infty}\tilde{G}(\tilde{\rho}_0)\int_0^a J_\ell(r\tilde{\rho}_0)J_\ell(r\tilde{\rho})r\mathrm{d}r\tilde{\rho}_0\mathrm{d}\tilde{\rho}_0 \quad (34)$$

Integrating over r, see p. 664 of [18], it reads

$$\mathcal{I}_{p,\ell}(\rho,z) = a^2\int_0^{\infty}\tilde{\rho}_0\tilde{G}(\tilde{\rho}_0)\frac{\left(\tilde{\rho}_r J_\ell(\tilde{\rho}_{0r})J_{\ell-1}(\tilde{\rho}_r) - \tilde{\rho}_{0r}J_{\ell-1}(\tilde{\rho_{0r}})J_\ell(\tilde{\rho}_r)\right)}{\tilde{\rho}_{0r}^2 - \tilde{\rho}_r^2}\mathrm{d}\tilde{\rho}_0 \quad (35)$$

with (see p. 706 of [18])

$$\tilde{G}(\tilde{\rho}_0) = \int_0^{\infty}G(\rho')J_\ell(\tilde{\rho}_0\rho')\rho'\mathrm{d}\rho' = \exp\left(-\frac{\tilde{\rho}_0^2}{8\alpha}\right)\frac{1}{\tilde{\rho}_0}\sum_{n=0}^{p}\frac{A_{p\ell}(n)}{\alpha^{n+\frac{\ell}{2}+\frac{1}{2}}}M_{n+\frac{\ell}{2}+\frac{1}{2},\frac{\ell}{2}}\left[-\frac{\tilde{\rho}_0^2}{4\alpha}\right]. \quad (36)$$

For simplicity, we assumed that $\ell \geq 0$. For $\ell < 0$, the identity $J_{-\ell}(X) = (-1)^\ell J_\ell(X)$ shows that the results would be identical up to a sign. We also use the explicit expression of $\mathrm{L}_p^\ell(X)$, see p. 1000 of [18], and define

$$A_{p\ell}(n) = E_0\frac{(-1)^n(p+\ell)!}{n!\ell!(p-n)!}\left(\frac{\sqrt{2}}{w_0}\right)^{2n+\ell} \quad (37)$$

As for the moments $\mu_m(p,\ell)$ of $\tilde{G}(\tilde{\rho}_0)$, we obtain [24]

$$\mu_m(p,\ell) = \pi 2^{m+1}\alpha^{\frac{m}{2}-\frac{\ell}{2}}\Gamma\left(1+\frac{m}{2}+\frac{\ell}{2}\right)\sum_{n=0}^{p}\frac{1}{\alpha^n}A_{p\ell}(n)\,{}_2F_1\left[1+\frac{m}{2}+\frac{\ell}{2},-n;\ell+1;1\right] \quad (38)$$

where ${}_2F_1[X]$ is the hypergeometric function, see p. 1005 of [18]. Performing the moment expansion of function $\tilde{G}(\tilde{\rho}_0)$ and integrating over $\tilde{\rho}_0$ one finally obtains

$$\mathcal{I}_{p,\ell}(\rho,z) = a^{\ell+2}\sum_{m=0}^{\infty}\frac{2^m}{m!}(a^2\alpha)^{\frac{m}{2}-\frac{\ell}{2}}\Gamma\left(1+\frac{m}{2}+\frac{\ell}{2}\right)\kappa_m(\tilde{\rho}_r)\sum_{n=0}^{p}\frac{1}{\alpha^n}A_{p\ell}(n){}_2F_1\left[1+\frac{m}{2}+\frac{\ell}{2},-n;\ell+1;1\right] \quad (39)$$

with, for $m > 0$

$$\kappa_m(\tilde{\rho}_r) = \frac{\partial^m}{\partial \tilde{\rho}_{0r}^m}\left(\frac{J_\ell(\tilde{\rho}_{0r})}{\tilde{\rho}_{0r}^2-\tilde{\rho}_r^2}\right)\Big|_{\tilde{\rho}_{0r}=0}\tilde{\rho}_r J_{\ell-1}(\tilde{\rho}_r) - \frac{\partial^m}{\partial \tilde{\rho}_{0r}^m}\left(\tilde{\rho}_{0r}\frac{J_{\ell-1}(\tilde{\rho}_{0r})}{\tilde{\rho}_{0r}^2-\tilde{\rho}_r^2}\right)\Big|_{\tilde{\rho}_{0r}=0} J_\ell(\tilde{\rho}_r) \quad (40)$$

and for $m = 0$, $\kappa_0(\tilde{\rho}_r) = -J_\ell(0)J_{\ell-1}(\tilde{\rho}_r)/\tilde{\rho}_r$, that is $\kappa_0(\tilde{\rho}_r) = 0$ for $\ell > 0$. Fixing $\ell = 0$ and $p = 0$ and using $J_{-1}(X) = -J_1(X)$, $A_{00}(0) = 1$ and ${}_2F_1\left[1+\frac{m}{2},0;1;1\right] = 1\,\forall m$, one can check that Eq. 39 gives, as expected, Eq. 18.

At first sight, the factor $\alpha^{\frac{m}{2}-\frac{\ell}{2}}$ of Eq. 39 may forbid to interpret this equation as a perturbation expansion for $\ell > 0$. However, calculating the derivatives terms of Eq. 40 we obtain for $m \geq \ell$ and ℓ and m integers of same parity:

$$\kappa_m(\tilde{\rho}_r) = \frac{m!}{2^{m+1}}\sum_{k=0}^{\frac{m-\ell}{2}}\frac{(-1)^k}{k!(k+\ell-1)!}\left(\frac{\tilde{\rho}_r}{2}\right)^{2k+\ell-m-2}\left[J_\ell(\tilde{\rho}_r) - \frac{\tilde{\rho}_r}{2(k+\ell)}J_{\ell-1}(\tilde{\rho}_r)\right] \quad (41)$$

and $\kappa_m(\tilde{\rho}_r) = 0$ if $m < \ell$ or ℓ and m integers of different parity. The first sum of Eq. 39 thus starts from $m = \ell$ so that this equation can be taken as a perturbation expansion in powers of α for $|\alpha| \lessapprox 1$. Expanding the Bessel functions in Eq. 41, we obtain an expression suitable for numerical calculations when $\tilde{\rho}_r$ is close to zero:

$$\kappa_m(\tilde{\rho}_r) = \frac{m!}{2^{m+1}}\sum_{k=0}^{\frac{m-\ell}{2}}\sum_{q=1+\frac{m-\ell}{2}}^{\infty}\frac{(-1)^{k+q}(k-q)}{k!q!(k+\ell)!(q+\ell)!}\left(\frac{\tilde{\rho}_r}{2}\right)^{2(k+\ell+q-1)-m} \quad (42)$$

From this expression one can eventually check that $\kappa_m(0) = 0\,\forall m$.

Eq. 39 can then finally be written

$$\mathcal{I}_{p,\ell}(\rho,z) = \mathcal{I}_{p,\ell}^{[\ell]}(\rho,z) + \sum_{\mu=1}^{\infty}\mathcal{I}_{p,\ell}^{[\mu]}(\rho,z) \quad (43)$$

with

$$\mathcal{I}_{p,\ell}^{[\ell]} = E_0 a^2\left(\frac{a\sqrt{2}}{w_0}\right)^\ell\frac{(p+\ell)!}{p!\ell!}\frac{J_{\ell+1}(\tilde{\rho}_r)}{\tilde{\rho}_r} \quad (44)$$

and

$$\mathcal{I}_{p,\ell}^{[\mu]}(\rho,z) = E_0 a^{\ell+2}\frac{2^{2\mu+\ell}(\mu+\ell)!}{(2\mu+\ell)!}(a^2\alpha)^\mu\kappa_{2\mu+\ell}(\tilde{\rho}_r)\sum_{n=0}^{p}\frac{1}{\alpha^n}A_{p\ell}(n)\,{}_2F_1\left[1+\mu+\ell,-n;\ell+1;1\right] \quad (45)$$

The first term of the perturbation expansion $\mathcal{I}_{p,\ell}^{[\ell]}$ corresponds to Fraunhofer approximation for $a/w_0 \to 0$. This expression has been previously derived and compared to experimental data [8].

However, Eq. 44 is in disagreement with Eq. 27 of [6] where $\mathcal{I}_{p,\ell}^{[\ell]} \propto J_{\ell+1}(\tilde{\rho}_r)/\tilde{\rho}_r^{\ell+1}$. No obvious misprint could be found to explain this disagreement. Therefore, since Eqs. 44 and 45 agree with numerical integration of Eq. 32 (see below), Eq. 27 of [6] is most likely affected by a non-trivial misprint or a calculation error.

Fig. 5 shows $\mathcal{I}_{p,\ell}(\rho)$ as a function of the dimensionless variable $a\tilde{\rho}$ for $p = 6$, $\ell = 3$. Twelve terms were needed in the sum over μ of Eq. 43 to reach a good agreement with the numerical integration of Eq. 32. The zeroth order contribution $\mathcal{I}_{p,\ell}^{[\ell]}$ is also shown for comparison. In order to show it on a similar scale as the result of the numerical integration, it has been multiplied by a factor 0.05. It has been checked that the three curves are superimposed when $a/w_0 = 0.05$ and $N_F \to 0$. As for the calculation precision, it is found to be similar to the one of section 3.A.

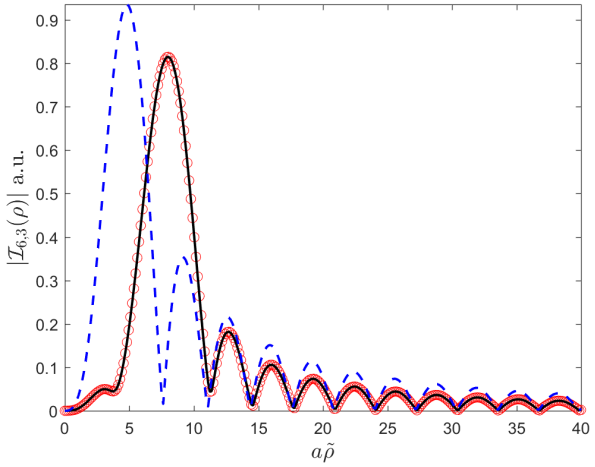

Fig. 5. $\mathcal{I}_{p,\ell}(\rho)$ as a function of the dimensionless variable $a\tilde{\rho}$ for $p = 6$, $\ell = 3$, $a = 1$, $N_F = 0.1$ and $a/w_0 = 1$. Full line : 13^{th} order (sum up to $\mu = 12$ in Eq. 43); circles: numerical integration (Eq. 32) ; dashed line: zeroth order contribution (multiplied by 0.05).

B. Near field region

As in section 3.B, we start with :

$$\mathcal{I}_{p,\ell}(\rho) = \mathcal{H}_\ell\left[\mathcal{H}_0[\tilde{f}(\tilde{\rho}_0)]G(\rho')\right] \quad (46)$$

with $\tilde{f}(\tilde{\rho}_0)$ and $G(r)$ defined in sections 3.B and 4.A respectively.

However, as in section 3.B, we have to account for the fact that the moments of $\tilde{f}(\tilde{\rho}_0)$ are undefined. We thus write

$$\mathcal{I}_{p,\ell}(\rho) = \int_0^\infty\left[\tilde{f}(\tilde{\rho}_0)\exp\left(-\frac{\tilde{\rho}_0}{4\alpha}\right)\right]\exp\left(\frac{\tilde{\rho}_0}{4\alpha}\right)J_0(r\tilde{\rho}_0)\int_0^\infty G(r)J_\ell(r\tilde{\rho})r\mathrm{d}r\tilde{\rho}_0\mathrm{d}\tilde{\rho}_0 \quad (47)$$

and perform the moment expansion of the term in the square bracket of the first integral. This expansion is indeed given by Eq. 25. Next, integrating over $\tilde{\rho}_0$, we obtain

$$\mathcal{I}_{p,\ell}(\rho) = \exp\left(-\frac{a^2\alpha}{2}\right)\sum_{N=0}^{\infty}M_{N,\frac{1}{2}}(a^2\alpha)\sum_{k=0}^{N}\frac{(-1)^k N!\alpha^k}{k!^2(N-k)!}\int_0^\infty G(r)J_\ell(r\tilde{\rho})r^{2k+1}\mathrm{d}r \quad (48)$$

Integrating over r and after some algebra, we finally obtain

$$\mathcal{I}_{p,\ell}(\rho) = \frac{E_0}{2\alpha}\exp\left(-\frac{a^2\alpha}{2}\right)\exp\left(-\frac{\tilde{\rho}^2}{4\alpha}\right)\left(\frac{\tilde{\rho}}{\alpha w_0\sqrt{2}}\right)^{\ell} \sum_{N=0}^{\infty} M_{N,\frac{1}{2}}(a^2\alpha)\sum_{q=0}^{p}\frac{(-1)^q(p+\ell)!}{(\ell+q)!(p-q)!}\left(\frac{2}{\alpha w_0^2}\right)^q \sum_{k=0}^{N}\frac{(-1)^k N!(q+k)!}{k!^2 q!(N-k)!}L_{q+k}^{\ell}\left(\frac{\tilde{\rho}^2}{4\alpha}\right) \quad (49)$$

This expression can be viewed as a perturbation expansion in powers of α^{-1} and therefore suitable to describe the near field region (*i.e* $N_F > 1$). It was checked that this expression gives Eq. 26 when $p = \ell = 0$.

As in section 3.B, the number of term to be retained in the sum over N of Eq. 49 increases when $a\rho$ increases. One needs typically 60 terms for $a\tilde{\rho} \leq 30$. To illustrate the agreement between Eq. 49 and the numerical integration of Eq. 32, a comparison is shown in fig. 6 for $p = 2$, $\ell = 1$, $N_F = 10$ and $w_0 = 4/5a$ with $a = 1$. For $a\rho \leq 50$, 100 terms where needed in the sum over N of Eq. 49. The zeroth order contribution is also shown. As for the calculation precision, it is found to behave similarly to the one of section 3.B.

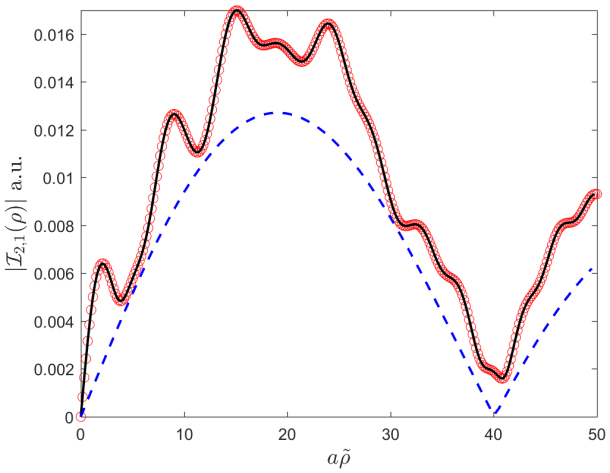

Fig. 6. $\mathcal{I}_{p,\ell}(\rho)$ as a function of the dimensionless variable $a\tilde{\rho}$ for $p = 2, \ell = 1, a = 1, N_F = 10$ and $a/w_0 = 5/4$. Full line : 100^{th} order (sum up to $N = 100$ in Eq. 49); Dashed line: zeroth order contribution ($N = 0$ in Eq. 49); circles: numerical integration (Eq. 32).

5. SUMMARY

A method based on the distribution theory has been used to compute Fresnel diffraction integrals. We specialized to Gaussian and Laguerre-Gauss beams and obtained useful expression for the near and far field regions. Interestingly, we have found that making a moment expansion of the Hankel transform of the incident field times the Fresnel propagator term leads to the diffracted far field. While expanding the Hankel transform of the screen aperture function, leads to the diffracted near field. Unfortunately, we have not been able to find a physical reason for describing this feature.

This method can be used to solve other diffraction problems. First, for the diffraction of Hermite-Gauss beam by a rectangular aperture, one just has to repeat the calculations presented in this article using Cartesian coordinates. Second, one can apply the results of this paper to the propagation of super-Gaussian beams. Indeed, these can be modeled by the convolution of a circular aperture function and a Gaussian beam [25], and the results of this article concerning Gaussian beams can be directly used. Third, the results can be extended to the diffraction by circular apertures of a slightly miss-aligned Gaussian beam. Such an incident beam can indeed be expended into a Hermite-Gauss series of modes [26]. Then, converting the transverse Cartesian coordinated into radial coordinates one obtains an expression that can be handled similarly to those of section 3. More speculatively, one could also look at the more precise diffraction integrals, e.g. Rayleigh-Sommerfeld diffraction formula [9]. The formal expressions of the Fourier or Hankel transform of the free-space Green function and its derivative [27] may allow to solve these integrals for particular cases.

DISCLOSURES

The authors declare no conflicts of interest.

DATA AVAILABILITY

No data were generated or analyzed in the presented research.

REFERENCES

1. Y. Shen, X. Wang, Z. Xie, C. Min, X. Fu, Q. Liu, M. Gong, and X. Yuan, "Optical vortices 30 years on: Oam manipulation from topological charge to multiple singularities," Light. Sci. & Appl. **8**, 1–29 (2019).
2. D. Hebri, S. Rasouli, and A. M. Dezfouli, "Theory of diffraction of vortex beams from structured apertures and generation of elegant elliptical vortex hermite–gaussian beams," J. Opt. Soc. Am. A **36**, 839–852 (2019).
3. M. A. Cruz-Gomez, D. López-Aguayo, and S. Lopez-Aguayo, "Two-dimensional solitons in laguerre–gaussian potentials," J. Opt. **22**, 015504 (2019).
4. T. Xia, D. Liu, A. Dong, G. Wang, H. Zhong, and Y. Wang, "Properties of partially coherent elegant laguerre-gaussian beam in free space and oceanic turbulence," Optik **201**, 163514 (2020).
5. J.-M. Rax and R. Gueroult, "Faraday–fresnel rotation and splitting of orbital angular momentum carrying waves in a rotating plasma," J. Plasma Phys. **87**, 1–22 (2021).
6. G. Lenz, "Far-field diffraction of truncated higher-order laguerre-gaussian beams," Opt. Commun. **123**, 423–429 (1996).
7. E. Cagniot, M. Fromager, and K. Ait-Ameur, "Adaptive laguerre-gaussian variant of the gaussian beam expansion method," J. Opt. Soc. Am. A **26**, 2373–2382 (2009).
8. A. Ambuj, R. Vyas, and S. Singh, "Diffraction of orbital angular momentum carrying optical beams by a circular aperture," Opt. Lett. **39**, 5475–5478 (2014).
9. J. W. Goodman, *Introduction to Fourier optics* (New York McGraw-Hill, 1999).
10. D. T. Gillespie, "Moment expansion representation of probability density functions," Am. J. Phys. **49**, 552–555 (1981).
11. G. Bekefi, "Diffraction of electromagnetic waves by an aperture in a large screen," J. applied physics **24**, 1123–1130 (1953).
12. N. Aoyagi and S. Yamaguchi, "Generalized fresnel transformations and their properties," Jpn. J. Appl. Phys. **12**, 1343–1350 (1973).
13. W. Southwell, "Validity of the fresnel approximation in the near field," JOSA **71**, 7–14 (1981).
14. S. Rasouli, A. M. Khazaei, and D. Hebri, "Talbot carpet at the transverse plane produced in the diffraction of plane wave from amplitude radial gratings," J. Opt. Soc. Am. A **35**, 55–64 (2018).
15. D. Hebri, S. Rasouli, and M. Yeganeh, "Intensity-based measuring of the topological charge alteration by the diffraction of vortex beams from

amplitude sinusoidal radial gratings," J. Opt. Soc. Am. B **35**, 724–730 (2018).
16. P. M. Morse and H. Feshbach, *Methods of theoretical physics Part I* (New York McGraw-Hill, 1953), p. 839.
17. G. E. Shilov, *Elementary real and complex analysis* (New York Dover, 1996), p. 497.
18. I. Gradshteyn and I. Ryzhik, *Table of integrals, series, and products* (Amsterdam Elsevier, 2007).
19. H. Kogelnik and T. Li, "Laser beams and resonators," Appl. optics **5**, 1550–1567 (1966).
20. M. Abramowitz and I. A. Stegun, *Hanbook of mathematical functions* (National Bureau of Standards Applied Mathematics Series 55, 1972), p. 508.
21. W. G. Rees, "The validity of the fresnel approximation," Eur. J. Phys. **8**, 44–48 (1987).
22. W. H. Southwell, "Validity of the fresnel approximation in the near field," J. Opt. Soc. Am. **71**, 7–14 (1981).
23. N. Baddour, "Operational and convolution properties of two-dimensional fourier transforms in polar coordinates," JOSA A **26**, 1767–1777 (2009).
24. A. Erdélyi, *Higher transcendental functions Vol. I* (New-York McGraw-Hill, 1953), p. 270.
25. S. Bollanti, P. Di Lazzaro, D. Murra, and A. Torre, "Analytical propagation of supergaussian-like beams in the far-field," Opt. Commun. **138**, 35–39 (1997).
26. D. Z. Anderson, "Alignment of resonant optical cavities," Appl. Opt. **23**, 2944–2949 (1984).
27. W. Chew, "A quick way to approximate a sommerfeld-weyl-type integral," IEEE Transactions on Antennas Propag. **36**, 1654–1657 (1988).